AUTHORS:
Mqhelewenkoso A. Mpofu[1]
Mlamuli Dhlamini[2]
Adolf Ndlovu[2]
Nqobile A. Chirwa[2]

AFFILIATIONS:
[1]Department of Mathematics and Statistics, Gwanda State University, Filabusi, Zimbabwe
[2]Department of Applied Mathematics, Faculty of Applied Science, National University of Science and Technology, Bulawayo, Zimbabwe

CORRESPONDENCE TO:
Mlamuli Dhlamini

EMAIL:
mlangeni2007@gmail.com

DATES:
Received: 25 Sep. 2024
Revised: 09 June 2025
Revised: 30 Sep. 2025
Accepted: 13 Nov. 2025
Published: 29 Jan. 2026

HOW TO CITE:
Mpofu MA, Dhlamini M, Ndlovu A, Chirwa NA. A two-dimensional Darcy–Forchheimer mathematical model for bioconvection flow with microbial exoprotein activity. S Afr J Sci. 2026;122(1/2), Art. #18964. https://doi.org/10.17159/sajs.2026/18964

ARTICLE INCLUDES:
☒ Peer review
☐ Supplementary material

DATA AVAILABILITY:
☐ Open data set
☐ All data included
☐ On request from author(s)
☐ Not available
☒ Not applicable

EDITOR:
Sydney Moyo

KEYWORDS:
exoprotein, bioconvection, microbes, spectral quasilinearisation method

FUNDING:
None

A two-dimensional Darcy–Forchheimer mathematical model for bioconvection flow with microbial exoprotein activity

Microbes play a pivotal role in heat and mass transfer in boundary layer flow. These microbes are added to nanofluids to promote efficiency and the desired fluid properties. Some microbes excrete exoproteins into the solution, which significantly affect chemical reactions, heat and mass transfer. Based on an extensive literature review, we found no models that consider the existence of exoprotein dynamics when modelling boundary layer flow. In our model, we developed a system of partial differential equations and included exoprotein dynamics. The system of partial differential equations was transformed into a system of ordinary differential equations and then solved numerically using the spectral quasilinearisation method to a high degree of accuracy. Our results show that thermophoresis and the Brownian motion parameters increase the exoprotein concentration. The increase in growth rate, carrying capacity, and exoprotein production rate causes a significant increase in exoprotein production, and eventually, the product increases. The degradation of the exoprotein decreases the product concentration. The increase in the growth rate and the thermophoresis parameters also causes the Nusselt number to increase.

Significance:

The action of enzymes drives chemical reactions in biological systems by producing specific protein molecules known as exoproteins. The effect of exoproteins is exploited in various industrial processes, including the brewing industry, pharmaceutical industry and, most recently, in mineral extraction. The current study investigates the fluid and flow dynamics of a nanofluid in the presence of microbes and exoproteins.

Introduction

The study of bioconvection flow is paramount in industrial processes and biomedical technology. Nanofluids and microbes play a significant role in enhancing the flow dynamics of momentum, heat and mass transfer, thereby improving the efficiency of the flow. Bioconvection is the directional collective swimming of microorganisms resulting in a macroscopic convection movement of the fluid.[1,2] Nanofluid is a term coined by Choi and Eastman[3] to describe fluids that contain nanosized particles to enhance certain key properties of the fluid for a specific desired function. Although Choi and Eastman received much recognition for the idea, Maxwell[4] was the first to attempt the technology. This attempt failed because the fluid passages clogged and damaged the pumps, a major setback in the commercialisation of the technology.[3,5,6] Typical nanoparticles usually consist of stable metals such as Al, Cu, Au, Ag and Fe oxides (namely Al_2O_3, CuO, TiO_2 and SiO_2), carbides (SiC), nitrides (AlN and SiN) or non-metals such as graphite and carbon nanotubes.[7,8] Typical base fluids are water, ethylene glycol (including other coolants), oil (including other lubricants), polymers, biofluids and conductive fluids.[7]

Motile microbes in porous media play a pivotal role in the bioconvection flow as they enhance the thermal efficiency of many systems.[9] The microbes can be any of the following: bacteria, fungi, algae, viruses, protozoa, etc. The microbes swim to the upper surface of the fluid and form a macroscopic, dense layer of microbes in the nanofluid, which becomes unstable.[10] Microbes are considered relatively less dense than water, resulting in bioconvection phenomena. They present an uneven and unstable structure due to self-propelled microbes swimming to the upper layer of the liquid, and this process of bioconvection flow occurs mainly with bacteria.[11] Microbe classification is based on their response to the type of stimulus, for example, gyrotactic, oxytactic, gravitactic or phototactic.[12] These microbes produce and actively secrete exoproteins.[13] Another microbial toxin class is endotoxins, which remain within the bacterial outer membrane. The idea of using exoproteins commercially is encountered in the brewing[14,15] and pharmaceutical industries[16-18]. In this study, we analysed the effects of the exoproteins on bioconvection flow. We aimed to develop a model that describes and predicts the effects of exoproteins on bioconvection flow. This study is significant considering the effect of exoproteins in cancer treatment when bacteria are exploited to kill advanced cancer cells or alter the function of the cells.[19,20] Exoproteins are also important in the manufacturing of vaccines and cheese production.[21,22] Ahmad et al.[12] developed a model that described exoprotein production, but no studies have modelled the bioconvection flow that included exoprotein production.

The current study is novel in that we are using two new aspects in heat and mass transfer models that are ignored in most models in the literature. Most models on bioconvection in the literature assume that the microbes are added constantly from the wall, ignoring the fact that they can grow in the culture. Furthermore, we investigated the dynamics of the proteins/enzymes excreted by these microbes, something that has been neglected in the past in the field of heat and mass transfer.

Mathematical model

We consider a two-dimensional bioconvection flow of an incompressible nanofluid flowing through a porous medium. The model includes the exoproteins whose concentration at the boundary is m_w and is proportional to the microbe's concentration n_w at the surface, that is, $m_w \propto n_w$. The exoprotein produces a solute (a chemical

product of interest) whose concentration is given by S and S_w is the concentration of the solute at the wall. T_w and C_w are considered the temperature and nanofluid concentration at the boundary, respectively.

$$\frac{\partial u}{\partial x}+\frac{\partial u}{\partial y}=0, \quad \text{Equation 1}$$

$$u\frac{\partial u}{\partial x}+v\frac{\partial u}{\partial y}=-\frac{1}{\rho}\frac{\partial p}{\partial x}+\nu\frac{\partial^2 u}{\partial y^2}-\frac{\sigma B_0^2}{\rho}u-\frac{\nu}{K}u-\frac{C_b}{x\sqrt{K}}u^2+(1-C_\infty)g\beta_T(T-T_\infty)-\frac{\rho_c-\rho}{\rho}g\beta_c(C-C_\infty)-\frac{\rho_n-\rho}{\rho}g\beta_n(n-n_\infty), \quad \text{Equation 2}$$

$$u\frac{\partial T}{\partial x}+v\frac{\partial T}{\partial y}=\alpha\left(1+\frac{16\sigma^* T_\infty^3}{3k\kappa^*}\right)\frac{\partial^2 T}{\partial y^2}+\frac{\nu}{C_p}\left(\frac{\partial u}{\partial y}\right)^2+\frac{\sigma B_0^2}{\rho C_p}u^2+\frac{\nu}{KC_p}u^2+\frac{C_b}{x\sqrt{K}}u^3+\tau\left(D_B\frac{\partial C}{\partial y}\frac{\partial T}{\partial y}+D_n\frac{\partial n}{\partial y}\frac{\partial T}{\partial y}+\frac{D_T}{T_\infty}\left(\frac{\partial T}{\partial y}\right)^2\right), \quad \text{Equation 3}$$

$$u\frac{\partial C}{\partial x}+v\frac{\partial C}{\partial y}=D_B\frac{\partial^2 C}{\partial y^2}+\frac{D_T}{T_\infty}\frac{\partial^2 T}{\partial y^2}, \quad \text{Equation 4}$$

$$u\frac{\partial n}{\partial x}+v\frac{\partial n}{\partial y}+\frac{bW_c}{\Delta C}\frac{\partial}{\partial y}\left(n\frac{\partial C}{\partial y}\right)=D_n\frac{\partial^2 n}{\partial y^2}+\frac{D_T}{T_\infty}\frac{\partial^2 T}{\partial y^2}+r(n-n_\infty)\left(1-\frac{n-n_\infty}{K_n\Delta n}\right), \quad \text{Equation 5}$$

$$u\frac{\partial m}{\partial x}+v\frac{\partial m}{\partial y}=D_m\frac{\partial^2 m}{\partial y^2}+\lambda(n-n_\infty)-\mu(m-m_\infty), \quad \text{Equation 6}$$

$$u\frac{\partial S}{\partial x}+v\frac{\partial S}{\partial y}=D_S\frac{\partial^2 S}{\partial y^2}+\frac{D_T}{T_\infty}\frac{\partial^2 T}{\partial y^2}+\lambda_s(m-m_\infty), \quad \text{Equation 7}$$

The associated boundary conditions are given as

$$\begin{aligned}&At\ y=0,\ u=cx,-\kappa_f\frac{\partial T}{\partial y}=h_f(T_w-T),\\&D_B\frac{\partial C}{\partial y}+\frac{D_T}{T_\infty}\frac{\partial T}{\partial y}=0,\ m=m_w,\ S=S_w,\\&-\kappa_n\frac{\partial n}{\partial y}=h_n(n_w-n).\\&At\ y\to\infty,\ u\to 0,\ \frac{\partial u}{\partial y}\to 0,\\&T\to T_\infty,\ C\to C_\infty,\ n\to n_\infty,\\&m\to m_\infty,\ S\to S_\infty.\end{aligned} \quad \text{Equation 8}$$

Here u is the velocity component along the x-axis and v is the velocity component along the y-axis, with y considered normal to the surface.[9] ρ is the fluid density, ρ_c is the nanoparticle density, ρ_n is the microbe density, ν is the kinetic viscosity, σ is the fluid conductivity and σ^* is the Stefan–Boltzmann constant, which refers to the electrical conductivity of the nanofluid. B_0 is the magnetic field, K is the permeability parameter, g is the gravitational acceleration, β_T is the thermal coefficient of expansion, β_C is the solute coefficient of expansion, β_n is the microbe coefficient of expansion, c_p is the specific heat capacity, C_b is the geometry-dependent drag coefficient, C and C_∞ are the nanoparticle concentration and ambient nanoparticle concentration, respectively, and n and n_∞ are the microbe concentration and ambient microbe, respectively. T and T_∞ are the temperature and ambient temperature, m and m_∞ are exoprotein and ambient exoprotein, D_B is the solute Brownian diffusion coefficient, D_T is the thermophoretic diffusion coefficient, D_m is the Brownian diffusion coefficient of the exoprotein, D_n is the Brownian diffusion coefficient of the microbe, κ is the thermal conductivity, $\propto$ is the thermal diffusivity, τ is the ratio of heat capacitance of nanoparticles to the base fluid, b is the chemotaxis constant, W_c is the maximum cell swimming speed, λ_n is the production rate of exoproteins, μ_m is the natural decay of the exoprotein and p is the pressure. $r(n-n_\infty)(1-(n-n_\infty)/\Delta nK_n)$ describes the logistic growth of microbes, where r is the microbial growth rate and K_n is the carrying capacity. Finally, h_f is the convective heat transfer coefficient, h_n is the microbe's transfer rate and κ_f is the conductivity of the fluid.

Transformation of partial differential equations

Dimensionless transformations are used to reduce the system of partial differential equations, Equations 2–7, and the boundary conditions, Equation 8, to obtain a system of ordinary differential equations. The transformations are given by

$$\begin{aligned}&\psi=\sqrt{c\nu}\,xf(\eta),\ \eta=y\sqrt{\frac{c}{\nu}},\ \theta(\eta)=\frac{T-T_\infty}{T_W-T_\infty},\\&\phi(\eta)=\frac{C-C_\infty}{C_W-C_\infty},\ \chi(\eta)=\frac{n-n_\infty}{n_W-n_\infty},\ \xi(\eta)=\frac{m-m_\infty}{m_W-m_\infty},\\&\varphi(\eta)=\frac{S-S_\infty}{S_W-S_\infty},\ u=cxf',\ v=-\sqrt{c\nu}\,f.\end{aligned} \quad \text{Equation 9}$$

The transformed equations are given by

$$f'''+ff''-Mf'-K_pf'-F_rf'^2+\frac{G_r}{Re^2}\left[\theta-N_r\phi-R_b\chi\right]=0, \quad \text{Equation 10}$$

$$\left(1+\frac{4}{3}R_d\right)\theta''+P_r\left[f\theta'+E_cf''^2+ME_cf'^2+K_pE_cf'^2+F_rE_cf'^3+N_b\theta'\phi'+N_n\chi'\theta'+N_t\theta'^2\right]=0, \quad \text{Equation 11}$$

$$\phi''+S_cf\phi'+\frac{N_t}{N_b}\theta''=0, \quad \text{Equation 12}$$

$$\chi''+S_bf\chi'-P_b[\phi'\chi'+\tau_\circ\phi''+\phi''\chi]+\frac{N_t}{N_n}\theta''+\tilde{r}S_b\chi\left(1-\frac{\chi}{K_n}\right)=0, \quad \text{Equation 13}$$

$$\xi''+S_d\left[f\xi'-A_2\xi+A_{1\chi}\right]=0, \quad \text{Equation 14}$$

$$\varphi''+S_s\left[f\varphi'+\tilde{\lambda}_s\xi\right]+\frac{N_t}{N_s}\theta''=0, \quad \text{Equation 15}$$

and the boundary conditions are given as

$$\begin{aligned}&f'(0)=1,f(0)=0,f'(\infty)\to 0,\ f''(\infty)\to 0,\\&\theta'(0)=-B_i(1-\theta(0)),\theta(\infty)\to 0,\\&N_b\phi'(0)+N_t\theta'(0)=0,\ \phi(\infty)\to 0,\\&\chi'(0)=-B_n(1-\chi(0)),\ \chi(\infty)\to 0,\\&\xi(0)=1,\ \xi(\infty)\to 0,\varphi(0)\to 1,\varphi(\infty)\to 0,\end{aligned} \quad \text{Equation 16}$$

where

$$F_r = \frac{C_b}{\sqrt{K}},\ K_p = \frac{\nu}{cK},\ Re = \frac{cx^2}{\nu},$$
$$G_r = \frac{g\beta_T(1-C_\infty)(T_w - T_\infty)}{\nu^2}x^3, M = \frac{\sigma\beta_\circ^2}{\rho c},$$
$$N_r = \frac{\beta_c(\rho_c - \rho)\Delta C}{\beta_T\rho(1-C_\infty)\Delta T},\ P_r = \frac{\nu}{\alpha},$$
$$R_b = \frac{\beta_n(\rho_n - \rho)\Delta n}{\beta_T\rho(1-C_\infty)\Delta T},\ E_c = \frac{(cx)^2}{c_p\Delta T},$$
$$S_c = \frac{\nu}{D_B},\ S_b = \frac{\nu}{D_n},\ R_d = \frac{4\sigma^* T_\infty^3}{\kappa\kappa^*},$$
$$N_b = \frac{\tau D_B \Delta C}{\nu},\ N_n = \frac{\tau D_n \Delta n}{\nu},\ \tau_\circ = \frac{n_\infty}{\Delta n},$$
$$N_s = \frac{\tau D_s \Delta S}{\nu},\ N_t = \frac{\tau D_T \Delta T}{\nu T_\infty},\ A_1 = \frac{\lambda\Delta n}{c\Delta m},$$
$$A_2 = \frac{\mu_m}{c},\ P_b = \frac{bW_c}{D_n},\ S_d = \frac{\nu}{D_m},$$
$$B_i = \frac{h_f}{\kappa_f}\frac{x}{\sqrt{Re}},\ B_n = \frac{h_n}{\kappa_n}\frac{x}{\sqrt{Re}},$$
$$S_s = \frac{\nu}{D_s},\ \tilde{\lambda}_s = \frac{\lambda_s\Delta m}{c\Delta S},\ \tilde{r} = \frac{r}{c}.$$

Equation 17

We define the parameters in Equations 10–16 as follows: M is the magnetic field parameter, Re is the Reynolds number (ratio of inertial forces to viscous forces), G_r is the Grashof number (ratio of buoyancy to viscous force), K_p is the permeability parameter, F_r is called the Forchheimer number, N_r is the buoyancy ratio parameter (ratio of thermal buoyancy to solute buoyancy), N_b is the Brownian motion parameter, which measures the random movement of particles in a fluid, N_n is the bioconvection Brownian motion parameter, which measures the random movement of microbes in a fluid, N_t is the thermophoresis parameter, which is a measure of the movement of microscopic particles due to a force of the temperature gradient, R_b is the bioconvection Rayleigh number (the ratio of thermal transport due to microorganisms to thermal transport via convection), E_c is the Eckert number, which measures the relationship between a flow's kinetic energy and the boundary layer enthalpy difference S_c is the Schmidt number (ratio of momentum diffusivity to mass diffusivity), S_b is the bioconvection Schmidt number (ratio of momentum diffusivity to microbes diffusivity), S_d is the Schmidt number (ratio of momentum diffusivity to exoprotein diffusivity), S_s is the Schmidt number for the solute (product), R_d is the thermal radiation (relative contribution of conduction heat transfer to thermal radiation transfer), P_r is the Prandtl number (ratio of momentum diffusivity to thermal diffusivity), P_b is the bioconvection Péclet number (ratio of the movement of microbes as a result of swimming to movement of microbes due to diffusion), τ_o is the constant microbial concentration difference parameter, τ_m is the constant exoprotein concentration difference parameter, A_1 is the exoprotein production rate by bacteria, A_2 is the natural degradation of exoprotein, λ_s is the production rate for the product "solute", B_i is the Biot number (thermal) and B_n is the Biot number (microbial).

Momentum, heat and mass coefficients

In this section, we consider the quantities that have an effect at the boundary, such as the local skin friction coefficient, the local Nusselt number, the Sherwood number and the local density number of microbes. The local skin friction coefficient (C_f) is given by

$$C_f = \frac{\tau_w}{\frac{1}{2}U_w^2} = -2\ Re^{-\frac{1}{2}}\ f''(0),$$ Equation 18

the local Nusselt number is given as

$$Nu_x = \frac{x\ q_w}{\kappa(T_w - T_\infty)} = -\left(1 + \frac{4}{3}Rd\right)Re^{\frac{1}{2}}\ \theta'(0),$$ Equation 19

the local Sherwood number is given as

$$Sh_x = \frac{x\ q_c}{D_B\ (C_w - C_\infty)} = -Re^{\frac{1}{2}}\phi'(0),$$ Equation 20

the local microbe density number is given as

$$Nn_x = \frac{x\ q_n}{D_n\ (n_w - n_\infty)} = -Re^{\frac{1}{2}}\chi'(0),$$ Equation 21

the local exoprotein density number is given as

$$Nm_x = \frac{x\ q_m}{D_m\ (m_w - m_\infty)} = -Re^{\frac{1}{2}}\xi'(0)$$ Equation 22

and the local product density number is given by

$$Ns_x = \frac{x\ q_s}{D_s\ (S_w - S_\infty)} = -Re^{\frac{1}{2}}\varphi'(0),$$ Equation 23

where

$$\tau_w = -\mu\frac{\partial u}{\partial y}\Big|_{y=0},\ q_w = \alpha\left(1 + \frac{4\ \sigma^* T_\infty^3}{3\kappa\kappa^*}\right)\frac{\partial T}{\partial y}\Big|_{y=0},$$
$$q_c = -D_B\frac{\partial C}{\partial y}\Big|_{y=0},\ q_n = -D_n\frac{\partial n}{\partial y}\Big|_{y=0},$$
$$q_m = -D_m\frac{\partial m}{\partial y}\Big|_{y=0},\ q_s = -D_s\frac{\partial S}{\partial y}\Big|_{y=0}.$$

Equation 24

Numerical simulation

The spectral quasilinearisation method involves transforming the domain $\eta \in [0,\ L_x]$ into the computational domain $z_i \in [-1,\ 1]$. The $N+1$ collocation points or grid points are generated from Gauss–Lobatto[23]

$$z_i = \cos\left(\frac{\pi i}{N}\right),\ i = 0,\ 1,\ 2,\ \ldots,\ N,$$ Equation 25

so that the grid points are given by

$$\eta_i = \frac{L_x(1+z_i)}{2},\ i = 0,\ 1,\ 2,\ \ldots,\ N.$$ Equation 26

By the spectral collocation method, we introduce the differentiation matrix D used to approximate derivatives of unknown variables (such as $f(\eta)$) at the collocation points such that

$$f' = \frac{df}{d\eta} = \sum_{j=0}^{N}\boldsymbol{D}_{ij}f(\eta_j) = Df,\ i = 0,\ 1,\ 2,\ \ldots,\ N,$$ Equation 27

where $\boldsymbol{D} = \frac{2D}{L_x}$ and

$$f = [f(z_o),\ f(z_1),\ \ldots,\ f(z_N)]$$ Equation 28

is the vector function at the collocation points.[23] This implies that

$$f^k = \boldsymbol{D}^k f, \quad \text{Equation 29}$$

where k is the order of the derivative.

The solution is approximated using the Lagrange interpolation polynomials of the form

$$u(\eta) = \sum_{i=0}^{N} \hat{u}(\eta_i) L_i(\eta), \quad \text{Equation 30}$$

where

$$L_i(\eta) = \prod_{i=0, j\neq k}^{N} \frac{\eta - \eta_i}{\eta_k - \eta_i}. \quad \text{Equation 31}$$

We also define Equations 10–15 using the functions F, Θ, Φ, ψ, X and Υ, respectively, such that

$$F = f''' + ff'' - Mf' - K_p f' - F_r f'^2 + \frac{G_r}{Re^2}\left[\theta - N_r\phi - R_b\chi\right], \quad \text{Equation 32}$$

$$\Theta = \left(1 + \frac{4}{3}R_d\right)\theta'' + P_r\left[f\theta' + E_c f'^2 + ME_c f'^2 + K_p E_c f'^2 + F_r E_c f'^3 + N_b\theta'\phi' + N_n\chi'\theta' + N_t\theta'^2\right], \quad \text{Equation 33}$$

$$\Phi = \phi'' + S_c f\phi' + \frac{N_t}{N_b}\theta'', \quad \text{Equation 34}$$

$$X = \chi'' + S_b f\chi' - P_b[\phi'\chi' + \tau_s\phi'' + \phi''\chi] + \frac{N_t}{N_n}\theta'' + \tilde{r}S_b\chi\left(1 - \frac{\chi}{K_n}\right), \quad \text{Equation 35}$$

$$\Upsilon = \xi'' + S_d\left[f\xi' - A_2\xi + A_1\chi\right], \quad \text{Equation 36}$$

$$\psi = \varphi'' + S_s\left[f\varphi' + \tilde{\lambda}_s\xi\right] + \frac{N_t}{N_s}\theta''. \quad \text{Equation 37}$$

Before constructing the iterative formula, we need to define the coefficients of the transformed variables:

$$a_{0r} = \frac{\partial F}{\partial f'''} = 1,\ a_{1r} = \frac{\partial F}{\partial f''} = f_r,$$
$$a_{2r} = \frac{\partial F}{\partial f'} = -\left(M + K_p + 2F_r f_r\right),$$
$$a_{3r} = \frac{\partial F}{\partial f} = f'',\ a_{4r} = \frac{\partial F}{\partial \theta} = \frac{G_r}{Re^2},$$
$$a_{5r} = \frac{\partial F}{\partial \phi} = -\frac{G_r N_r}{Re^2},\ a_{6r} = \frac{\partial F}{\partial \chi} = -\frac{G_r R_b}{Re^2},$$
$$b_{0r} = \frac{\partial \Theta}{\partial \theta''} = 1 + \frac{4}{3}R_d,$$
$$b_{1r} = \frac{\partial \Theta}{\partial \theta'} = P_r f_r + P_r N_b \phi_r' + P_r N_n \chi_r' + 2P_r N_t \theta_r',$$
$$b_{2r} = \frac{\partial \Theta}{\partial f''} = 2P_r E_c f_r'',$$
$$b_{3r} = \frac{\partial \Theta}{\partial f'} = 2P_r M E_c f_r' + 2P_r K_P E_c f_r' + 3P_r F_r E_c f_r'^2,$$
$$b_{4r} = \frac{\partial \Theta}{\partial f} = P_r\theta_r',\ b_{5r} = \frac{\partial \Theta}{\partial \phi'} = P_r N_b \theta_r',$$
$$b_{6r} = \frac{\partial \Theta}{\partial \chi'} = P_r N_n \theta_r'$$
$$c_{0r} = \frac{\partial \Phi}{\partial \phi''} = 1,\ c_{1r} = \frac{\partial \Phi}{\partial \phi'} = S_c f_r,$$
$$c_{2r} = \frac{\partial \Phi}{\partial f} = S_c\phi'',\ c_{3r} = \frac{\partial \Phi}{\partial \phi''} = \frac{N_t}{N_b}$$

$$d_{0r} = \frac{\partial X}{\partial \chi''} = 1,\ d_{1r} = \frac{\partial X}{\partial \chi'} = S_b f_r - P_b\phi_r',$$
$$d_{2r} = \frac{\partial X}{\partial \chi} = -P_b\phi_r'' + \tilde{r}S_b\left(1 - \frac{2\chi_r}{K_n}\right),\ d_{3r} = \frac{\partial X}{\partial f} = S_b\chi_r',$$
$$d_{4r} = \frac{\partial X}{\partial \theta''} = \frac{N_t}{N_n},\ d_{5r} = \frac{\partial X}{\partial \phi''} = -P_b(\tau_o + \chi_r),\ d_{6r} = \frac{\partial X}{\partial \phi'} = -P_b\chi_r',$$
$$e_{0r} = \frac{\partial \Upsilon}{\partial \xi''} = 1,\ e_{1r} = \frac{\partial \Upsilon}{\partial \xi'} = S_d f_r,\ e_{2r} = \frac{\partial \Upsilon}{\partial \xi} = S_d A_2,$$
$$e_{3r} = \frac{\partial \Upsilon}{\partial f} = S_d\xi_r',\ e_{4r} = \frac{\partial \Upsilon}{\partial \chi} = S_d A_1,$$
$$h_{0r} = \frac{\partial \psi}{\partial \varphi''} = 1,\ h_{1r} = \frac{\partial \psi}{\partial \varphi'} = S_s f_r,\ h_{2r} = \frac{\partial \psi}{\partial f} = S_s\varphi_r',$$
$$h_{3r} = \frac{\partial \psi}{\partial \theta''} = \frac{N_t}{N_s},\ h_{4r} = \frac{\partial \psi}{\partial \xi} = S_s\tilde{\lambda}_s.$$

Equation 38

We then define the residuals and also construct the iterative formula for the system of equations:

$$a_{0r}f_{r+1}''' + a_{1r}f_{r+1}'' + a_{2r}f_{r+1}' + a_{3r}f_{r+1} + a_{4r}\theta_{r+1} + a_{5r}\phi_{r+1} + a_{6r}\chi_{r+1} - F = R_f, \quad \text{Equation 39}$$

$$b_{0r}\theta_{r+1}'' + b_{1r}\theta_{r+1}' + b_{2r}f_{r+1}'' + b_{3r}f_{r+1}' + b_{4r}f_{r+1} + b_{5r}\phi_{r+1}' + b_{6r}\chi_{r+1}' - \Theta = R_\Theta, \quad \text{Equation 40}$$

$$c_{0r}\phi_{r+1}'' + c_{1r}\phi_{r+1}' + c_{2r}f_{r+1} + c_{3r}\theta_{r+1}'' - \Phi = R_\Phi, \quad \text{Equation 41}$$

$$d_{0r}\chi_{r+1}'' + d_{1r}\chi_{r+1}' + d_{2r}\chi_{r+1} + d_{3r}f_{r+1} + d_{4r}\theta_{r+1}'' + d_{5r}\phi_{r+1}'' + d_{6r}\phi_{r+1}' - X = R_X, \quad \text{Equation 42}$$

$$e_{0r}\xi_{r+1}'' + e_{1r}\xi_{r+1}' + e_{2r}\xi_{r+1} + e_{3r}f_{r+1} + e_{4r}\chi_{r+1} - \Upsilon = R_\Upsilon, \quad \text{Equation 43}$$

$$h_{0r}\varphi_{r+1}'' + h_{1r}\varphi_{r+1}' + h_{2r}f_{r+1} + h_{3r}\theta_{r+1}'' + h_{4r}\xi_{r+1} - \psi = R_\psi, \quad \text{Equation 44}$$

where R is the residual term for velocity (R_f), temperature (R_θ), nanoparticles (R_Φ), microbes (R_X), exoprotein (R_Υ) and solute product (R_ψ).

The iterative boundary conditions are given by

$$f_{r+1}'(0) = 1,\ f_{r+1}(0) = 0,\ f_{r+1}'(\infty) \to 0,$$
$$f_{r+1}''(\infty) \to 0,\ \theta_{r+1}'(0) = -B_i\left(1 - \theta_{r+1}(0)\right),\ \theta_{r+1}(\infty) \to 0,$$
$$N_b\phi_{r+1}'(0) + N_t\theta_{r+1}'(0) = 0,\ \phi_{r+1}(\infty) \to 0, \quad \text{Equation 45}$$
$$\chi_{r+1}'(0) = -B_n\left(1 - \chi_{r+1}(0)\right),\ \chi_{r+1}(\infty) \to 0,\ \xi_{r+1}(0) = 1,$$
$$\xi_{r+1}(\infty) \to 0,\ \varphi_{r+1}(0) \to 1,\ \varphi_{r+1}(\infty) \to 0.$$

Assume that f_o, θ_o, ϕ_o, χ_o, ξ_o and φ_o are initial guesses such that

$$f_o(\eta) = 1 - e^{-\eta},\ \theta_o(\eta) = \frac{B_i}{1 + B_i}e^{-\eta},$$
$$\phi_o(\eta) = -\frac{N_t}{N_b}\frac{B_i}{1 + B_i}e^{-\eta}, \quad \text{Equation 46}$$
$$\chi_o(\eta) = \frac{B_n}{1 + B_n}e^{-\eta},\ \xi_o(\eta) = e^{-\eta},$$
$$\varphi_o(\eta) = e^{-\eta}.$$

Applying Equation 31, we have

$$(a_{0r}D^3 + a_{1r}D^2 + a_{2r}D + a_{3r}I)f_{r+1} + (a_{4r}I)\theta_{r+1} + (a_{5r}I)\phi_{r+1} + (a_{6r}I)\chi_{r+1} = R_f, \quad \text{Equation 47}$$

$$(b_{2r}D^2 + b_{3r}D + b_{4r}I)f_{r+1} + (b_{0r}D^2 + b_{1r}D)\theta_{r+1} + (b_{5r}D)\phi_{r+1} + (a_{6r}D)\chi_{r+1} = R_\Theta, \quad \text{Equation 48}$$

$$(c_{2r}I)f_{r+1} + (c_{3r}D^2)\theta_{r+1} + (c_{0r}D^2 + c_{1r}D)\phi_{r+1} + 0\chi_{r+1} + 0\xi_{r+1} + 0\varphi_{r+1} = R_\Phi, \quad \text{Equation 49}$$

$$(d_{3r}I)f_{r+1} + (d_{4r}D^2)\theta_{r+1} + (d_{5r}D^2 + d_{6r}D)\phi_{r+1} + (d_{0r}D^2 + d_{1r}D + d_{2r}I)\chi_{r+1} = R_X, \quad \text{Equation 50}$$

$$(e_{3r}D)f_{r+1} + 0\theta_{r+1} + 0\phi_{r+1} + (e_{4r}I)\chi_{r+1} + (e_{0r}D^2 + e_{1r}D + e_{2r}I)\xi_{r+1} = R_\xi, \quad \text{Equation 51}$$

$$(h_{2r}I)f_{r+1} + (d_{3r}D^2)\theta_{r+1} + 0\phi_{r+1} + 0\chi_{r+1} + (h_{4r}I)\xi_{r+1} + (h_{0r}D^2 + h_{1r}D)\varphi_{r+1} = R_\psi, \quad \text{Equation 52}$$

Equations 46–51 can be written in matrix form as

$$\begin{bmatrix} A_{11} & A_{12} & A_{13} & A_{14} & A_{15} & A_{16} \\ A_{21} & A_{22} & A_{23} & A_{24} & A_{25} & A_{26} \\ A_{31} & A_{32} & A_{33} & A_{34} & A_{35} & A_{36} \\ A_{41} & A_{42} & A_{43} & A_{44} & A_{45} & A_{46} \\ A_{51} & A_{52} & A_{53} & A_{54} & A_{55} & A_{56} \\ A_{61} & A_{62} & A_{63} & A_{64} & A_{65} & A_{66} \end{bmatrix} \begin{bmatrix} f_{r+1} \\ \theta_{r+1} \\ \phi_{r+1} \\ \chi_{r+1} \\ \xi_{r+1} \\ \varphi_{r+1} \end{bmatrix} = \begin{bmatrix} R_f \\ R_\Theta \\ R_\Phi \\ R_X \\ R_\chi \\ R_\psi \end{bmatrix}, \quad \text{Equation 53}$$

where

$$\begin{aligned} &A_{11} = a_{0r}D^3 + a_{1r}D^2 + a_{2r}D + a_{3r}I, \\ &A_{12} = a_{4r}I,\ A_{13} = a_{5r}I,\ A_{14} = a_{6r}I, \\ &A_{15} = 0,\ A_{16} = 0,\ A_{21} = b_{2r}D^2 + b_{3r}D + b_{4r}I, \\ &A_{22} = b_{0r}D^2 + b_{1r}D,\ A_{23} = b_{5r}D,\ A_{24} = a_{6r}D, \\ &A_{25} = 0,\ A_{26} = 0,\ A_{31} = c_{2r}I,\ A_{32} = c_{3r}D^2, \\ &A_{33} = c_{0r}D^2 + c_{1r}D,\ A_{34} = 0,\ A_{35} = 0, \\ &A_{36} = 0,\ A_{41} = d_{3r}I,\ A_{42} = d_{4r}D^2, \\ &A_{43} = d_{5r}D^2 + d_{6r}D,\ A_{44} = d_{0r}D^2 + d_{1r}D + d_{2r}I, \\ &A_{45} = 0,\ A_{46} = 0,\ A_{51} = e_{3r}D,\ A_{52} = 0,\ A_{53} = 0, \\ &A_{54} = e_{4r}I,\ A_{55} = e_{0r}D^2 + e_{1r}D + e_{2r}I,\ A_{56} = 0, \\ &A_{61} = h_{2r}I,\ A_{62} = d_{3r}D^2,\ A_{63} = 0,\ A_{64} = 0, \\ &A_{65} = h_{4r}I,\ A_{66} = h_{0r}D^2 + h_{1r}D. \end{aligned} \quad \text{Equation 54}$$

Results and discussion

Table 1 gives the values of the parameters used for the simulations and their sources. To validate the accuracy of the numerical scheme, we performed a residual error analysis. The results of the residual error analysis are given in Table 2 and Figure 1. Our errors are of the order of 10^{-12} to 10^{-10}, which means our scheme is very accurate. In Table 3, we present the study of the effect of some key parameters of interest on the fluid and flow properties. A parameter is varied over three values, and the corresponding values are recorded to see how the parameter affects the local skin friction, Nusselt number, Sherwood number, microbes, exoprotein and product density.

Figure 2 presents the effect of magnetic field parameters on different variables in the model. The application of a magnetic field produces a drag force that leads to a reduction in the velocity of the fluid, which is accompanied by an increase in all other species within the boundary layer. Similar results are found in the literature.[36-38] The exoprotein and product are also shown to increase at the boundary layer for increasing values of the magnetic field.

Table 1: Parameter values and sources

Parameter	Symbol	Value	Reference
Magnetic field	M	(0, 6)	24,25
Permeability	K_p	0.2	26
Forchheimer number	F_r	0.5	27
Grashof number	G_r	(0.1, 1)	26
Reynolds number	Re	1	26
Buoyancy ratio	N_r	(0.3, 1.2)	28
Bioconvection Rayleigh number	R_b	0.1	8
Thermal radiation	R_d	0.3	9
Prandtl number	P_r	0.72	27
Eckert number	E_c	(0.1, 3)	29
Brownian motion	N_b	(0.1, 5)	30
Thermophoresis	N_t	(0.1, 0.5)	6,30
Microbe's Brownian motion	N_n	0.5	31
Schmidt number	S_c	3.4	31
Bioconvection Schmidt number	S_d	3.4	Assumed
Bioconvection Péclet number	P_b	(0.1, 1.0)	9,32
Microbial difference constant	τ_o	0.2	8
Microbial growth rate	r	0.1	33
Carrying capacity	K_n	10	Assumed
Schmidt number for the protein	S_d	3.4	Assumed
Schmidt number for the product	S_s	3.4	Assumed
Exoprotein production rate	A_1	0.2	34
Natural degradation of exoprotein	A_2	0.1	Assumed
Production rate for the product	λ_s	0.9	Assumed
Biot number (thermal)	B_i	(0.1, 50)	24,35
Biot number (microbial)	B_n	(0.1, 50)	Assumed

In Figure 3, we present the effect of the microbial Brownian motion parameter on different model variables. The microbe concentration decreases with increasing values of this parameter. Similar results for this phenomenon were presented by Dhlamini et al.[6] The exoprotein and product also decrease with an increase in the microbes' Brownian motion parameter. This is because these are directly dependent on the microbes, resulting in a decrease in the microbes. This, in turn, leads to a decrease in exoproteins and products. Temperature and fluid velocity increase with an increase in the microbes' Brownian motion parameter. Dhlamini et al.[6] obtained similar results for the temperature profile. Gorla et al.[39] reached similar conclusions for solute Brownian motion.

In Figures 4, 5 and 6, we study the effect of the microbial growth rate parameter, carrying capacity, rate of production of the product and

Table 2: Residual errors

i	$f(\eta)$	$\theta(\eta)$	$\phi(\eta)$	$\chi(\eta)$	$\xi(\eta)$	$\varphi(\eta)$
1	$4.52879190 \times 10^{-09}$	$2.48885357 \times 10^{-11}$	$2.98805425 \times 10^{-12}$	$1.89686045 \times 10^{-11}$	$4.66642003 \times 10^{-12}$	$1.75433622 \times 10^{-11}$
2	$2.30051267 \times 10^{-09}$	$5.62727642 \times 10^{-12}$	$3.44213547 \times 10^{-12}$	$6.90081325 \times 10^{-12}$	$5.01332309 \times 10^{-12}$	$1.15610854 \times 10^{-11}$
3	$3.69907971 \times 10^{-09}$	$1.67381664 \times 10^{-11}$	$4.39359660 \times 10^{-12}$	$1.16373577 \times 10^{-11}$	$5.10451403 \times 10^{-12}$	$2.86101143 \times 10^{-11}$
4	$1.31282119 \times 10^{-09}$	$1.42612588 \times 10^{-11}$	$3.60267371 \times 10^{-12}$	$1.06941123 \times 10^{-11}$	$5.74022774 \times 10^{-12}$	$1.46910817 \times 10^{-11}$
5	$1.89027927 \times 10^{-09}$	$1.24300570 \times 10^{-11}$	$4.64073224 \times 10^{-12}$	$1.65438774 \times 10^{-11}$	$6.08341155 \times 10^{-12}$	$1.27341471 \times 10^{-11}$
6	$3.15445683 \times 10^{-10}$	$2.46913601 \times 10^{-11}$	$4.51194637 \times 10^{-12}$	$1.28380639 \times 10^{-11}$	$5.21832577 \times 10^{-12}$	$1.54740110 \times 10^{-11}$
7	$4.22095026 \times 10^{-09}$	$2.02327044 \times 10^{-11}$	$3.43169937 \times 10^{-12}$	$7.41717798 \times 10^{-12}$	$4.05986356 \times 10^{-12}$	$2.35455266 \times 10^{-11}$
8	$6.56893429 \times 10^{-10}$	$1.12234666 \times 10^{-11}$	$1.33004718 \times 10^{-12}$	$6.43274323 \times 10^{-12}$	$6.89298618 \times 10^{-12}$	$1.53696778 \times 10^{-11}$
9	$7.16446458 \times 10^{-10}$	$1.18538512 \times 10^{-11}$	$5.67790259 \times 10^{-12}$	$6.94899693 \times 10^{-12}$	$4.72447081 \times 10^{-12}$	$1.26509359 \times 10^{-11}$
10	$8.59152749 \times 10^{-10}$	$1.48197010 \times 10^{-11}$	$3.07043280 \times 10^{-12}$	$1.49379398 \times 10^{-11}$	$2.51314941 \times 10^{-12}$	$1.60303160 \times 10^{-11}$

Table 3: Effect of varying key parameters on local skin friction $f''(0)$, Nusselt number $\theta'(0)$, Sherwood number $\Phi'(0)$, microbe density parameter $\chi'(0)$, exoprotein density parameter $\xi'(0)$ and product density parameter $\varphi'(0)$

N_t	r	A_1	A_2	$f''(0)$	$\theta'(0)$	$\phi'(0)$	$\chi'(0)$	$\xi'(0)$	$\varphi'(0)$
0.2	0.2	0.2	0.1	-2.28480140	0.08472393	-0.12711554	-0.11929443	-0.57749971	1.95304268
0.3				-2.28363583	0.09009348	-0.19502897	-0.07848386	-0.39091858	2.54242381
0.4				-2.28227248	0.09512741	-0.26553031	-0.04548963	-0.21920718	3.10752997
0.5				-2.28072172	0.09986325	-0.33844447	-0.01947548	-0.06190059	3.64600057
0.3	0.05			-2.27936819	0.07884141	-0.18563390	–0.31857071	–1.01332285	1.01443160
	0.1			-2.27999671	0.08010380	–0.18665849	–0.28907304	–0.93121467	1.23931874
	0.2			-2.28363583	0.09009348	–0.19502897	–0.07848386	–0.39091858	2.54242381
	0.3			-2.29748898	0.13657905	–0.23488280	0.83715733	1.98578069	8.05432909
	0.2	0.1		-2.28363583	0.09009349	–0.19502899	–0.07848364	–0.79012017	1.48245432
		0.15		-2.28363583	0.09009348	–0.19502897	–0.07848386	–0.59051948	2.01243891
		0.2		-2.28363583	0.09009348	–0.19502897	–0.07848386	–0.39091858	2.54242381
		0.25		-2.28363583	0.09009348	–0.19502897	–0.07848386	–0.19131768	3.07240871
		0.2	0.1	-2.28363583	0.09009349	–0.19502899	–0.07848362	–0.39091813	2.54242449
			0.15	-2.28363583	0.09009348	–0.19502897	–0.07848386	–0.54240660	2.23927221
			0.2	-2.28363583	0.09009348	–0.19502897	–0.07848386	–0.67328678	1.99496115
			0.25	-2.28363583	0.09009348	–0.19502897	–0.07848386	–0.78890232	1.79342183

exoprotein degradation rate. Increasing the bacterial growth rate and carrying capacity leads to an increase in the microbe population[33], which, in turn, increases the exoprotein and the product. The temperature also increases, as increasing the microbes' population increases the microbial Brownian motion. The solute concentration is shown to decrease with an increase in these parameters. The mechanism that drives the phenomenon is not clear at this point. An increase in exoprotein production rate is noted to have a significant effect on the product profile. The product increases significantly with an increase in the exoprotein rate.[13] Protein strains enhance the quality of products. For example, in cheese production, proteins play an important role in determining the texture and quality of the cheese by promoting the proteolysis process and the production of bioactive peptides.[40]

Conclusion

In this article, we have formulated a model to capture the dynamics of momentum, heat and mass transfer in the porous medium flow of a nanofluid with the effect of microbial activity. The current study extended the microbial activities to include the microbial growth and secretion of

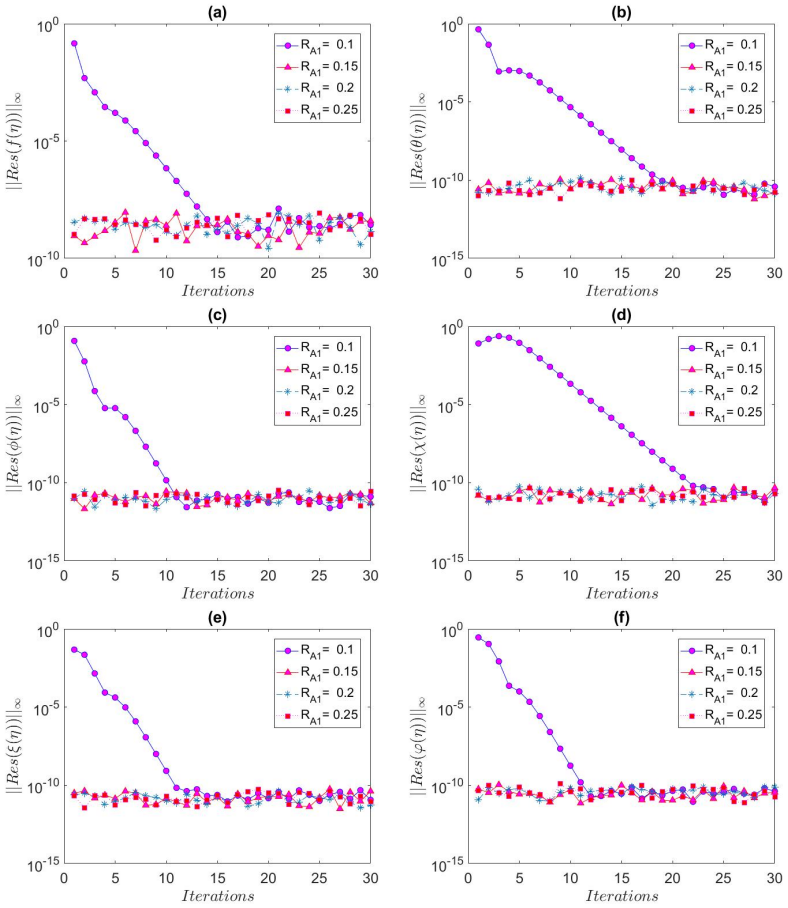

Figure 1: Residual errors: (a) velocity, (b) temperature, (c) nanoparticles, (d) microbes, (e) exoprotein and (f) product.

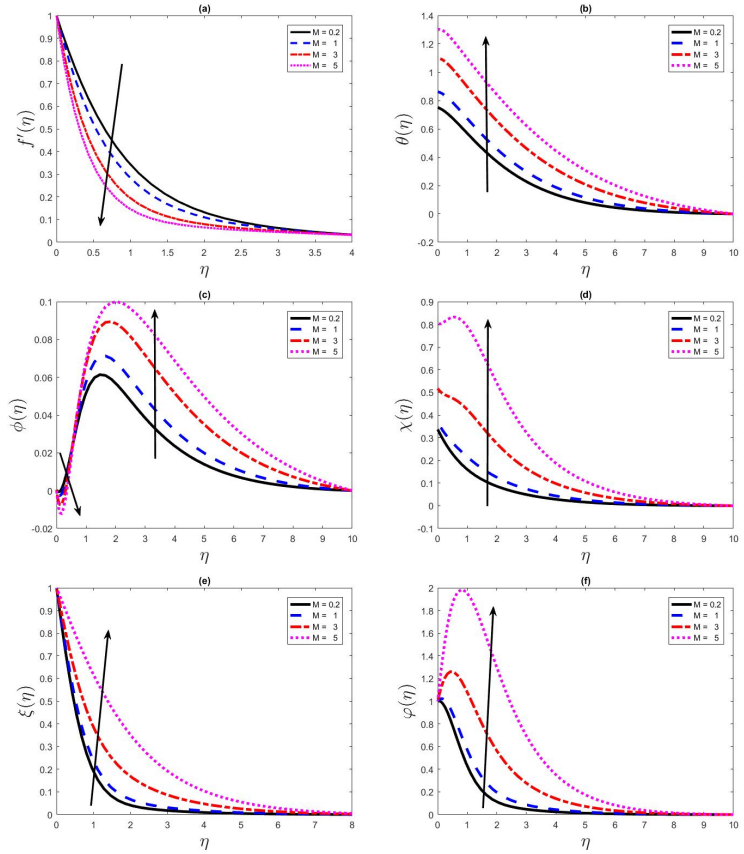

Figure 2: Effect of magnetic field parameters on (a) velocity, (b) temperature, (c) nanoparticles, (d) microbes, (e) exoprotein and (f) product.

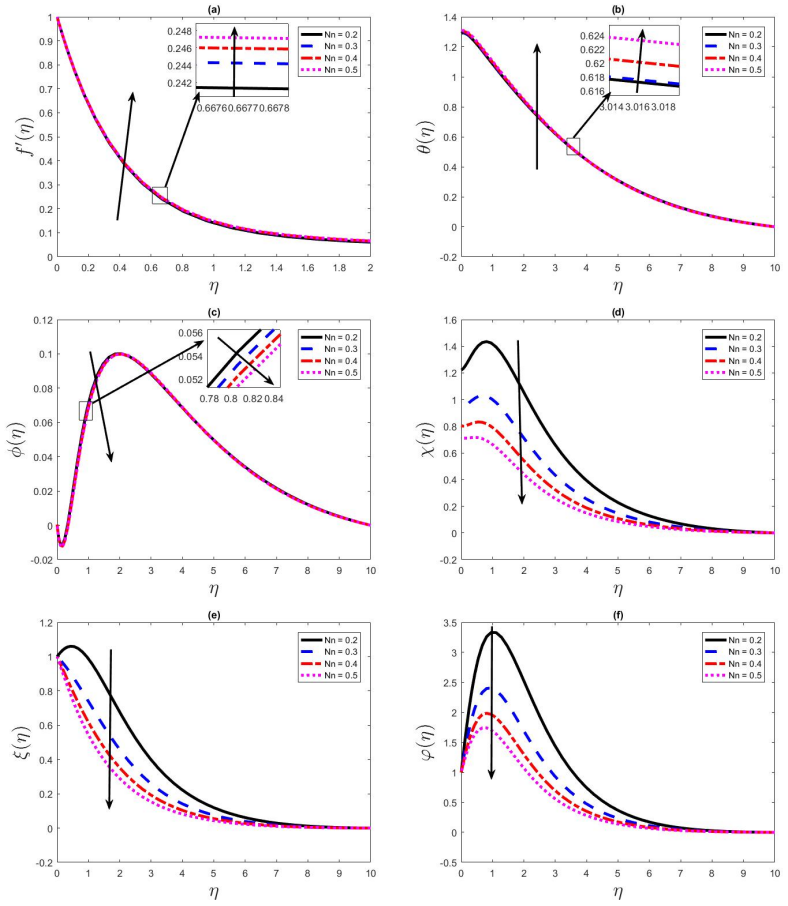

Figure 3: Effect of microbe Brownian motion on (a) velocity, (b) temperature, (c) nanoparticles, (d) microbes, (e) exoprotein and (f) product.

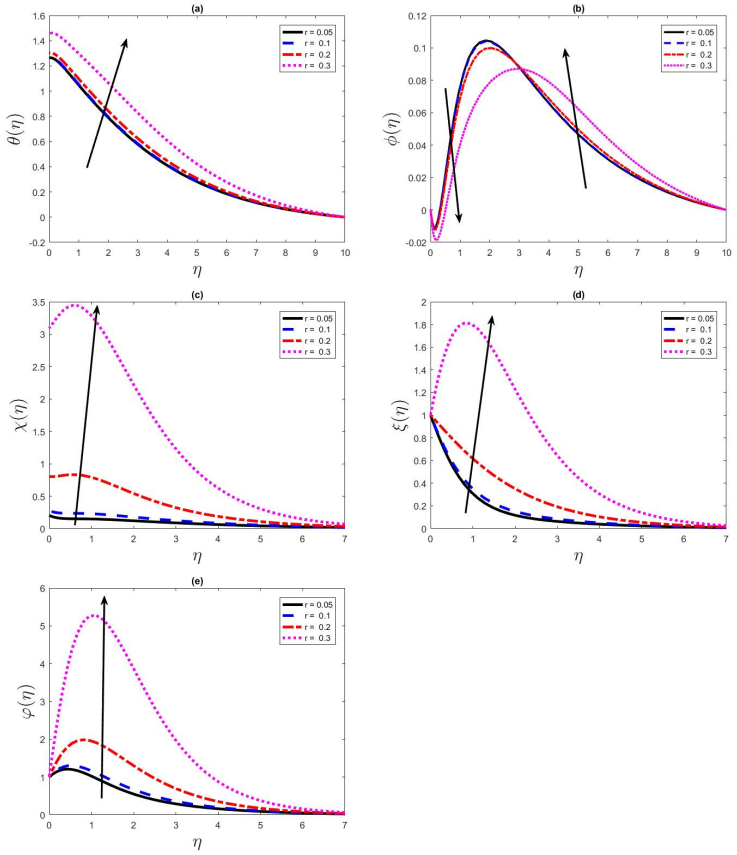

Figure 4: Effect of growth rate on (a) temperature, (b) nanoparticles, (c) microbes, (d) exoprotein and (e) product.

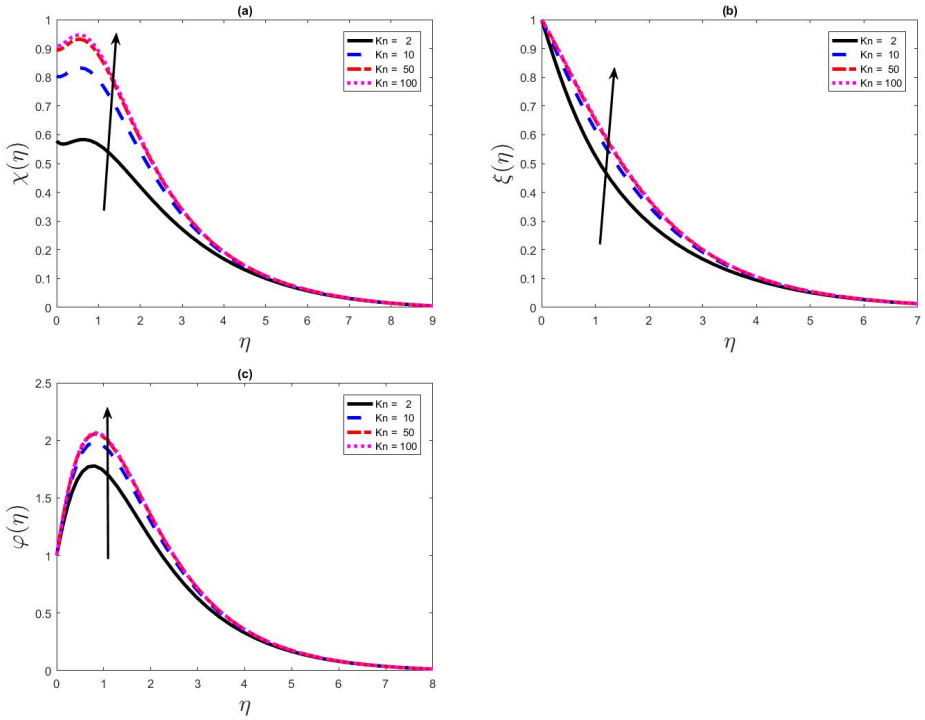

Figure 5: Effect of carrying capacity on (a) microbes, (b) exoprotein and (c) product.

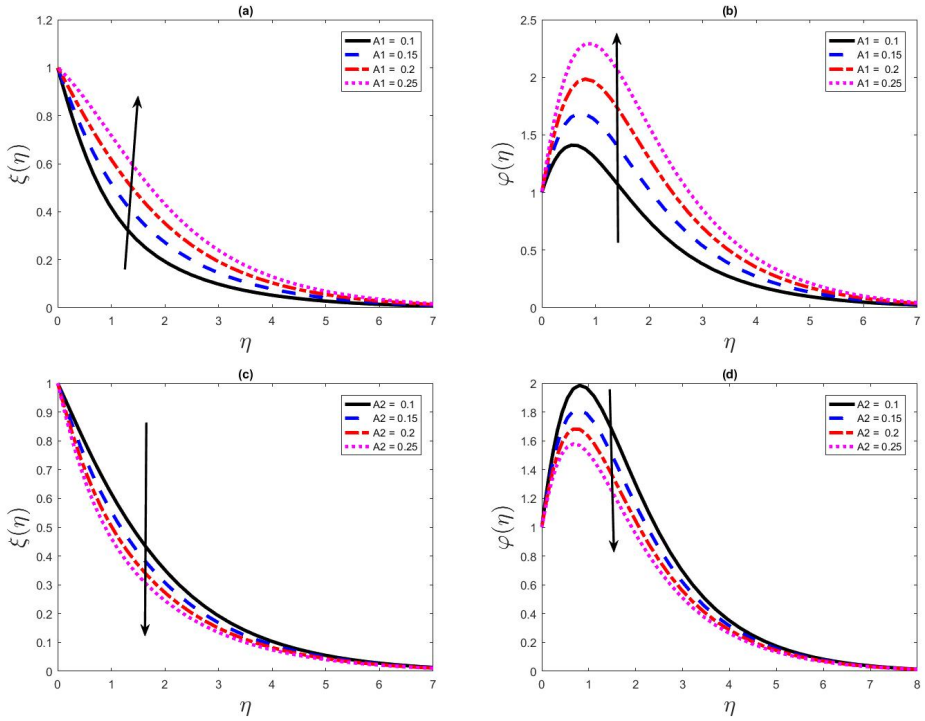

Figure 6: Effect of exoprotein production and degradation rate parameters: (a) production rate of microbes, (b) production rate of product, (c) degradation rate of microbes and (d) degradation rate of product.

exoproteins that are used in different industrial technologies, such as in the pharmaceutical industry. The following important observations were deduced from the study:

- The magnetic field parameter retards the fluid velocity, leading to a decrease in the convective transport and, thus, an increase in all other species is observed.
- Although the mechanism is unknown, the growth rate parameter increases with temperature whilst reducing the nanoparticle concentration close to the wall.
- The microbe's Brownian motion parameter increases with temperature and fluid velocity whilst reducing the microbes, exoproteins and product concentration.

Data availability

All data generated or analysed during the study are included in this published article.

Declarations

We have no competing interests to declare. We have no AI or LLM use to declare. This paper is adapted from a master's dissertation by M.A.M., supervised by M.D. and submitted to the Department of Applied Mathematics at the National University of Science and Technology (Zimbabwe) for an MSc in Applied Mathematics Modelling.

Authors' contributions

M.A.M.: Methodology, investigation, formal analysis, validation, numerical analysis, writing – original draft, writing – review and editing. M.D.: Conceptualisation, methodology, investigation, formal analysis, validation, numerical analysis, supervision, writing – original draft, writing – review and editing. A.N.: Methodology, investigation, formal analysis, validation, numerical analysis, writing – original draft, writing – review and editing. N.A.C.: Methodology, investigation, formal analysis, validation, numerical analysis, writing – original draft, writing – review and editing. All authors read and approved the final manuscript.

References

1. Platt JR. "Bioconvection patterns" in cultures of free-swimming organisms. Science. 1961;133(3466):1766–1767. https://doi.org/10.1126/science.133.3466.1766
2. Ferdows M, Zaimi K, Rashad AM, Nabwey HA. MHD bioconvection flow and heat transfer of nanofluid through an exponentially stretchable sheet. Symmetry. 2020;12(5), Art. #692. https://doi.org/10.3390/sym12050692
3. Choi SUS, Eastman JA. Enhancing thermal conductivity of fluids with nanoparticles. Technical report. Lemont, IL: Argonne National Lab; 1995.
4. Maxwell JC. A treatise on electricity and magnetism. Vol. 1. Oxford: Clarendon Press; 1873.
5. Lee J, Mudawar I. Assessment of the effectiveness of nanofluids for single-phase and two-phase heat transfer in micro-channels. Int J Heat Mass Transf. 2007;50(3–4):451–463. https://doi.org/10.1016/j.ijheatmasstransfer.2006.08.001
6. Dhlamini M, Zondo K, Mondal H, Sibanda P, Shaw S, Motsa SS, et al. Secondgrade bioconvection flow of a nanofluid with slip convective boundary conditions. Pramana-J Phys. 2023;97(4), Art. #197. https://doi.org/10.1007/s12043-023-02676-0
7. Mutuku WN, Makinde OD. Hydromagnetic bioconvection of nanofluid over a permeable vertical plate due to gyrotactic microorganisms. Comput Fluids. 2014;95:88–97. https://doi.org/10.1016/j.compfluid.2014.02.026
8. Dhlamini M, Mondal H, Sibanda P, Motsa S. Rotational nanofluids for oxytactic microorganisms with convective boundary conditions using bivariate spectral quasi-linearization method. J Cent South Univ. 2020;27(3):824–841. https://doi.org/10.1007/s11771-020-4334-x
9. Ahmad S, Ashraf M, Ali K. Bioconvection due to gyrotactic microbes in a nanofluid flow through a porous medium. Heliyon. 2020;6(12), e05832. https://doi.org/10.1016/j.heliyon.2020.e05832
10. Fathollahi R, Alizadeh A, Safari Y, Nabi H, Shamsborhan M, Taghinia F. Examination of bio convection with nanoparticles containing microorganisms under the influence of magnetism fields on vertical sheets by five-order Runge–Kutta method. Heliyon. 2023;9(5), e15982. https://doi.org/10.1016/j.heliyon.2023.e15982
11. Kada B, Hussain I, Pasha AA, Khan WA, Tabrez M, Juhany KA, et al. Significance of gyrotactic microorganism and bioconvection analysis for radiative Williamson fluid flow with ferromagnetic nanoparticles. Therm Sci Eng Prog. 2023;39, Art. #101732. https://doi.org/10.1016/j.tsep.2023.101732
12. Ahmad S, Younis J, Ali K, Rizwan M, Ashraf M, Abd El Salam MA. Impact of swimming gyrotactic microorganisms and viscous dissipation on nanoparticles flow through a permeable medium: A numerical assessment. J Nanomater. 2022;2022, Art. #4888128. https://doi.org/10.1155/2022/4888128
13. Coleman KD, Fowler AC. A mathematical model of exoprotein production in bacteria. Math Med Biol. 1984;1(1):77–94. https://doi.org/10.1093/imammb/1.1.77
14. Bokulich NA, Bamforth CW. The microbiology of malting and brewing. Microbiol Mol Biol Rev. 2013;77(2):157–172. https://doi.org/10.1128/MMBR.00060-12
15. Roselli GE, Kerruish DWM, Crow M, Smart KA, Powell CD. The two faces of microorganisms in traditional brewing and the implications for no-and low-alcohol beers. Front Microbiol. 2024;15, Art. #1346724. https://doi.org/10.3389/fmicb.2024.1346724
16. Santos-Beneit F. What is the role of microbial biotechnology and genetic engineering in medicine? MicrobiologyOpen. 2024;13(2), e1406. https://doi.org/10.1002/mbo3.1406
17. Chunduri A, Donthula N, Jahanavi M, Golla S, Aich P, Sahithya K, et al. Role of microbes in the pharmaceutical industry. In: Kumar S, Kumar N, Shahid-ul-Islam S, editors. Role of microbes in industrial products and processes. Hoboken, NJ: John Wiley & Sons; 2022. https://doi.org/10.1002/9781119901198.ch1
18. Ali MZ. Role of microorganism in pharmaceutical industry [document on the Internet]. c2013 [cited 2024 Sep 25]. https://doi.org/10.13140/RG.2.1.4671.0883
19. Zahaf NI, Schmidt G. Bacterial toxins for cancer therapy. Toxins. 2017;9(8), Art. #236. https://doi.org/10.3390/toxins9080236
20. Weerakkody LRN, Witharana C. The role of bacterial toxins and spores in cancer therapy. Life Sci. 2019;235, Art. #116839. https://doi.org/10.1016/j.lfs.2019.116839
21. Schmitt CK, Meysick KC, O'Brien AD. Bacterial toxins: Friends or foes? Emerg Infect Dis. 1999;5(2), Art. #224. https://doi.org/10.3201/eid0502.990206
22. Melkonian C, Zorrilla F, Kjarbolling I, Blasche S, Machado D, Junge M, et al. Microbial interactions shape cheese flavour formation. Nat Commun. 2023;14(1), Art. #8348. https://doi.org/10.1038/s41467-023-41059-2
23. Motsa SS, Dlamini PG, Khumalo M. Spectral relaxation method and spectral quasilinearization method for solving unsteady boundary layer flow problems. Adv Math Phys. 2014;2014, Art. #341964. https://doi.org/10.1155/2014/341964
24. Dhlamini M, Mondal H, Sibanda P, Motsa S. Activation energy and entropy generation in viscous nanofluid with higher-order chemically reacting species. Int J Ambient Energy. 2022;43(1):1495–1507. https://doi.org/10.1080/01430750.2019.1710564
25. Dhlamini M, Zondo K, Duve P, Mondal H, Mishra S, Sibanda P, et al. Cattaneo-Christov heat flux-based micropolar nanofluid flow with relaxation, slip, and temperature jump effects. Results Eng. 2024;23, Art. #102645. https://doi.org/10.1016/j.rineng.2024.102645
26. Dhlamini M, Kameswaran PK, Sibanda P, Motsa S, Mondal H. Activation energy and binary chemical reaction effects in mixed convective nanofluid flow with convective boundary conditions. J Comput Des Eng. 2019;6(2):149–158. https://doi.org/10.1016/j.jcde.2018.07.002
27. Mburu ZM, Mondal S, Sibanda P. Numerical study on combined thermal radiation and magnetic field effects on entropy generation in unsteady fluid flow past an inclined cylinder. J Comput Des Eng. 2021;8(1):149–169. https://doi.org/10.1093/jcde/qwaa068
28. Pal D, Mondal H. The influence of thermal radiation on hydromagnetic Darcy–Forchheimer mixed convection flow past a stretching sheet embedded in a porous medium. Meccanica. 2011;46:739–753. https://doi.org/10.1007/s11012-010-9334-8
29. Makinde OD, Sibanda P. Effects of chemical reaction on boundary layer flow past a vertical stretching surface in the presence of internal heat generation. Int J Numer Methods Heat Fluid Flow. 2011;21(6):779–792. https://doi.org/10.1108/09615531111148509
30. Sithole H, Mondal H, Sibanda P. Entropy generation in a second grade magnetohydrodynamic nanofluid flow over a convectively heated stretching sheet with nonlinear thermal radiation and viscous dissipation. Results Phys. 2018;9:1077–1085. https://doi.org/10.1016/j.rinp.2018.04.003

31. Alsaedi A, Razaq A, Hayat T, Khan SA. On bioconvective chemically reactive flow involving applications of magnetohydrodynamic and radiation. Alexandria Eng J. 2023;75:549–563. https://doi.org/10.1016/j.aej.2023.06.015

32. Imran M, Farooq U, Waqas H, Anqi AE, Safaei MR. Numerical performance of thermal conductivity in bioconvection flow of cross nanofluid containing swimming microorganisms over a cylinder with melting phenomenon. Case Stud Therm Eng. 2021;26, Art. #101181. https://doi.org/10.1016/j.csite.2021.101181

33. Allen RJ, Waclaw B. Bacterial growth: A statistical physicist's guide. Rep Prog Phys. 2018;82(1), Art. #016601. https://doi.org/10.1088/1361-6633/aae546

34. Horska K, Vankova J, Šebesta K. Determination of exotoxin in bacillus thuringiensis cells. Zeitschrift Naturforschung C. 1975;30(1–2):120–123. https://doi.org/10.1515/znc-1975-1-224

35. Olanrewaju PO, Arulogun OT, Adebimpe K. Internal heat generation effect on thermal boundary layer with a convective surface boundary condition. Am J Fluid Dyn. 2012;2(1):1–4. https://doi.org/10.5923/j.ajfd.20120201.01

36. Dhlamini M, Mondal H, Sibanda P, Mosta SS, Shaw S. A mathematical model for bioconvection flow with activation energy for chemical reaction and microbial activity. Pramana. 2022;96(2), Art. #112. https://doi.org/10.1007/s12043-022-02351-w

37. Dhlamini M, Mondal H, Sibanda P, Motsa S. Spectral quasi-linearization methods for Powell–Eyring MHD flow over a nonlinear stretching surface. J Nanofluids. 2018;7(5):917–927. https://doi.org/10.1166/jon.2018.1503

38. Misra S, Kamatam G. Effect of magnetic field, heat generation and absorption on nanofluid flow over a nonlinear stretching sheet. Beilstein J Nanotechnol. 2020;11(1):976–990. https://doi.org/10.3762/bjnano.11.82

39. Gorla RSR, Chamka AJ, Rashad AM. Mixed convective boundary layer flow over a vertical wedge embedded in a porous medium saturated with nanofluid: Natural convection dominated regime. Nanoscale Res Lett. 2011;6, Art. #207. https://doi.org/10.1186/1556-276X-6-207

40. Bouroutzika E, Proikakis S, Anagnostopoulos AK, Katsafadou AI, Fthenakis GC, Tsangaris GT. Proteomics analysis in dairy products: Cheese, a review. Appl Sci. 2021;11(16), Art. #7622. https://doi.org/10.3390/app11167622